EurJIC
European Journal of Inorganic Chemistry

A Journal of ChemPubSoc Europe

Accepted Article

Title: A precious catalyst: Rhodium-catalyzed formic acid dehydrogenation in water

Authors: Cornel Fink and Gabor Laurenczy

To be cited as: *Eur. J. Inorg. Chem.* 10.1002/ejic.201900344

Link to VoR: http://dx.doi.org/10.1002/ejic.201900344

WILEY-VCH

WILEY-VCH

FULL PAPER

A precious catalyst: Rhodium-catalyzed formic acid dehydrogenation in water

Cornel Fink* and Gábor Laurenczy*[a]

Abstract: The rhodium complex [Cp*Rh(bis(pyrazol-1-yl)methane)Cl]Cl was evaluated about its performance towards formic acid dehydrogenation in aqueous solution. The solid-state X-ray diffraction helped to confirm the catalyst structure. Multinuclear NMR spectroscopy was employed to follow the dehydrogenation of formic acid. The reactions have been carried out in high-pressure NMR sapphire tubes. An activation energy of +77.19 ± 4 kJ/mol was determined via an Arrhenius plot, which is in good agreement with literature findings. The catalyst afforded a TOF of 1086 h^{-1} and exhibited good stability. Based on our observations and literature, we propose a catalytic cycle.

Introduction

The Daily Mail released in 2018 an article entitled “Earth's glaciers have passed the point of no return: Study warns melting over the next 100 YEARS cannot be stopped even if emissions are slashed“.[1] Despite this strongly discouraging statement, it is emphasized that our current attempts to limit the exhaust of greenhouse gases (GHG) will make a difference in 100 years. The main factors for increasing global energy consumption is an ever-growing world population and increasing living standards. Primary energy supply is mainly achieved by the combustion of fossil fuels, a process which releases infrared active gases into the atmosphere, where they contribute to a phenomenon known as global warming.[2] Emission-free renewable energy production driven by sun and wind is an attractive alternative to the prevalent system. A significant drawback associated with sun- and wind-powered energy generation is its unsteady nature. A performant energy storage and release system can help to overcome this shortcoming.[3] The electrolysis of water transforms electricity into hydrogen, a chemical energy carrier that can be converted back to electricity via fuel cell technology. Intermediate hydrogen storage on an industrial scale is nowadays done by compression or liquefaction. Both methods are energy intensive, and safety requirements are strict when dealing with cryogenic liquids or highly pressurized cylinders.[4]

Besides using physical principles to store hydrogen, chemical approaches are a viable alternative. Some solutions propose the reversible hydrogenation of aromatic systems,[5] also hydrogen-rich compounds such as boron hydrides[6] could serve as hydrogen storage media.[7] Another promising approach is to bind hydrogen reversibly to a cheap and abundant carrier molecule to obtain liquid organic hydrogen carriers (LOHC).[8] The catalytic reduction of carbon dioxide (CO_2) yields formic acid (FA), a LOHC with a high volumetric hydrogen content (53 g/L), readily biodegradable and liquid at room temperature.[3b, 9] Sustainable formic acid production is accessible via catalytic CO_2 hydrogenation.[10] Hydrogen liberation from FA works with a 100% storage efficiency when conducted with an appropriate catalyst and at moderate temperatures.[3a, 11] Together, these two reactions form the formic acid/carbon dioxide cycle as schematically shown in (Figure 1). On this basis, hydrogen fuel stations could be realized as was proposed by Müller *et al*.[12]

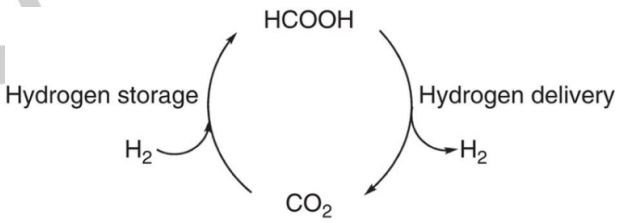

Figure 1 The formic acid/carbon dioxide cycle for reversible hydrogen storage[10]

In many scenarios, the reaction is performed in water, a benign and green solvent, but many other well-working solvent systems are known to literature,[13] including the direct dehydrogenation of neat FA.[14] The continuous attempts to elucidate the mode of operation of various catalysts give detailed insight into the mechanistic processes during the reaction.[15]

Numerous platinum group metal complexes with various ligands can catalyze the reaction. Especially prolific are bidentate nitrogen donor ligands,[15b, 15f, 16] phosphine containing structures,[10] and pincer ligands.[13d, 17] However, for a large-scale application, first-row transition metal catalysts are more attractive, for many reasons but mainly because they are cheap and abundant. The development of working iron catalysts is an essential step in this direction.[18] Also, ruthenium catalysts were intensively studied and the research afforded a series of reliable and stable catalysts, which are even active in CO_2 hydrogenation.[8b, 10, 19] Recent reviews on the topic are available.[8a, 20] Reaction solvents and additives play a crucial role in catalytic systems. Especially basic additives (triethylamine) are often employed to shift the thermodynamic equilibrium of systems.[21] Due to their frequent application, we assess the effects with calorimetric and spectroscopic methods.[22] Heterogeneous catalysts like heterogenized complexes,[23] and nanoparticles[24] have also been proven to be active in the

[a] Dr. C. Fink, Prof. G. Laurenczy
Institut des Sciences et Ingénierie Chimiques
École Polytechnique Fédérale de Lausanne (EPFL)
CH-1015 Lausanne (Switzerland)
Fax : (+41)21-693-9780
E-mail: fink.cornel@gmail.com , gabor.laurenczy@epfl.ch

Supporting information for this article is given via a link at the end of the document.

hydrogen storage/delivery in the formic acid/carbon dioxide couple, as reviewed by Himeda *et al*.[25]

The combination of a metal with cyclopentadienyl (Cp) is a common motif in the organometallic synthesis, and a large number of renowned compounds exhibit this structural feature such as ferrocene[26] or ruthenocene.[27] While earlier publications often deal with Cp compounds, more recent research regularly reports on pentamethylcyclopentadienyl (Cp*). Cp* offers several advantages over Cp, beginning with the fact that it can be stored conveniently since it does not undergo Diels Alder dimerization.[28] In mechanistic terms, the electron density of Cp*, imparted by the inductive effect of the methyl groups, is - compared to unsubstituted Cp - increased and contributes in general to an enhanced crystallizability and protection of the metal against reduction.[29] Furthermore, the steric expansion of Cp* exerts a protective effect on the metal center and limits the accessibility of other ligands and substrate from this side. The negative charge of cyclopentadienyl improves the solubility in polar solvents; especially the solvation in aqueous media is improved in compared to uncharged arene analogs. Powerful catalysts for CO_2 hydrogenation and formic acid dehydrogenation of the type [Cp*Ir(III)(N,N')Cl]Cl are reported in the literature.[16a, 30] Also the production of methanol was achieved with a [Cp*Ir(N,N')] catalyst.[8a, 31] Rhodium found much less attention for this application despite it displays excellent catalytic performance in many reactions [32] and Shriver *et.al* mention a working homogeneous catalyst for FA dehydrogenation in the seventies.[33] Here, we developed a catalytic system for selective formic acid dehydrogenation to hydrogen and carbon dioxide based on a rhodium complex (Figure 2). One advantage of Rh over iridium is that is NMR active, a property which could be exploited for elucidating mechanistic aspects.

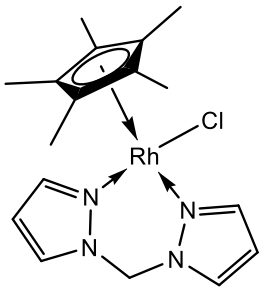

*Figure 2 Rh precatalyst (**3**)*

Results and Discussion

The precatalyst (Figure 2) is easily accessible via microwave synthesis of the dinuclear precursor $[Cp^*RhCl_2]_2$ and subsequent ligation of *bis(pyrazol-1-yl)methane* (dpm). The structure of the precatalyst was confirmed by X-ray crystallography (Figure 3). dpm shows for the two homotopic hydrogen atoms on the bridging carbon one signal at 6.29 ppm (s, 2 H in $CDCl_3$) in proton spectra when measured as a pure compound. However, when it binds as a ligand, the hydrogens appear at different chemical shifts. The crystal structure shows that the ligand binds via two nitrogen atoms to the metal center, locking the ligand in place, and exposing the hydrogen atoms (peaks labeled with **2** in Figure 4) to different chemical environments (6.70 ppm (dd, J = 14.7, 3.8 Hz, 1H) and 5.92 ppm (dd, J = 14.8, 3.7 Hz, 1H) Figure 4). The compound is well soluble in aqueous formic acid solutions.

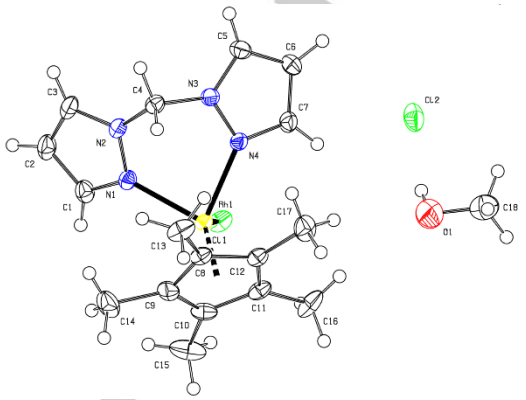

*Figure 3 Crystal structure of [Cp*Rh(bis(pyrazol-1-yl)methane)Cl]Cl; recrystallized from MeOH at RT as single clear pale orange prism-shaped crystals*

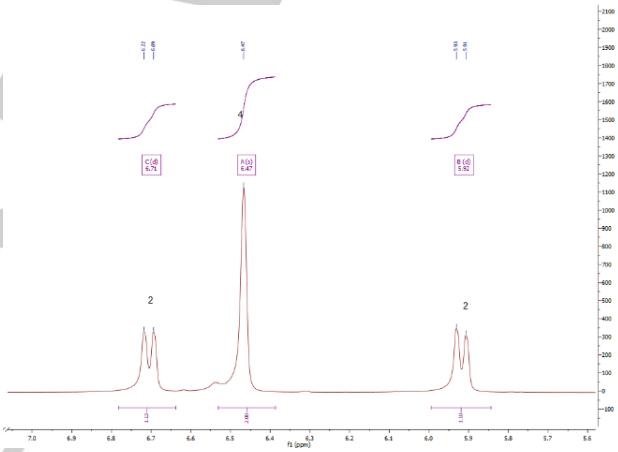

*Figure 4 ^{1}H-spectrum of [Cp*Rh(bis(pyrazol-1-yl)methane)Cl]Cl in $CDCl_3$ (full spectrum see SI)*

The catalytic activity was assessed by dehydrogenating 2.46 M aqueous formic acid solutions that were equivalent to 0.222 g pure formic acid. Two orthogonal techniques were used to follow the process. NMR spectroscopy was used to record time-resolved spectra. Therefore, the dehydrogenation reaction was performed in sealed sapphire tubes inside the NMR instrument, allowing us to monitor the reaction progress continuously. Figure 5 shows stacked proton spectra of a FA dehydrogenation reaction. Formic acid appears as a singlet at 8.40 ppm. During the dehydrogenation process, the peak shifts slightly high field while slowly fading away. The variation of the chemical shift during the experiment can be attributed to the changing pH values, decreasing FA concentrations.[22, 34] The catalyst promotes, as a side-reaction, also the exchange of the none-acidic C**H** proton of FA with deuterium atoms of the solvent. This process contributes to a small extent to the disappearance of the signal in proton NMR spectra. Proton-deuterium exchange is also a reason why hydride signals are often more difficult to detect when the reaction is conducted in heavy water.

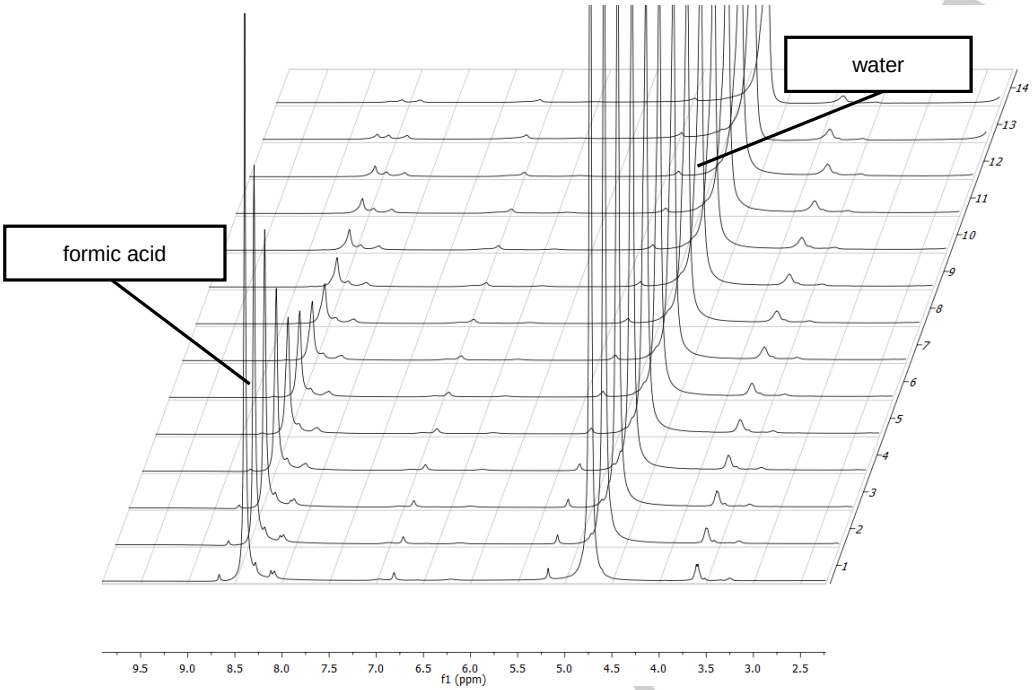

Figure 5 1H NMR (400 MHz, 10 mm) stacked spectra; 2.46 M FA in D2O at 70°C; formic acid dehydrogenation; c(Rh) = 0,01 M;

However, the dehydrogenation reaction occurs much faster than the exchange reaction. ^{1}H-NMR measurements support the findings that the catalyst is capable of selective formic acid dehydrogenation. No carbon monoxide could be detected in the formed H_2 + CO_2 gas mixture (detection limit < 5 ppm).

Knowing about the effects of proton-deuterium exchange processes, we performed a dehydrogenation experiment with carbon-13 labeled formic acid and recorded carbon spectra (SI-Figure S1). The doublet at 165.48 ppm (first scan) is formic acid as the only signal. After setting the temperature to 95°C, a new peak evolves at 125.0 ppm (spectrum 2), which is $^{13}CO_2$. Between spectrum 7/8, the doublet is almost completely gone while a triplet becomes apparent after the 5th spectrum (δ 165.91 ppm). This was assigned to DCOOH. Interestingly, the signal originating from the isotope-exchanged formic acid remains throughout the whole duration of the experiment. Even on a spectrum, recorded after 15 hours of reaction time, the triplet was still present, while normal FA (H^{13}COOH) could only be detected in traces at 167.19 and 165.03 ppm (Figure 6). The presence of these signals is not unexpected since the experiment was carried out in a pressured environment (final pressure 60 bar at RT CO_2:H_2, 1:1). Under these conditions, CO_2 can, in presence of a suitable catalyst, undergo hydrogenation back to formic acid. Overall, the findings suggest that $HCOO^-$ is more readily dehydrogenated than $DCOO^-$.

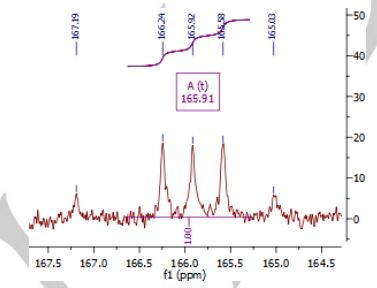

Figure 6 Signal of D13COOH (165.91 ppm); the two accompanying signals to the left and the right of the triplet are traces of H13COOH;

Pressure measurements were the second technique to follow the dehydrogenation progress. Formic acid dehydrogenation releases hydrogen and carbon dioxide in equal amounts in moles; the pressure increase in a sealed vessel over time is proportional to the progression of the reaction. The reaction is completed, in equilibrium, when there is no more pressure increase (Figure 7). Depending on the reaction temperature and the volume of the tube, the total pressure inside the reaction vessel can rise up to almost 90 bar. The ligands coordinated around the metal center must protect it against direct reduction through molecular hydrogen. We used the final pressure readings for our calculations.

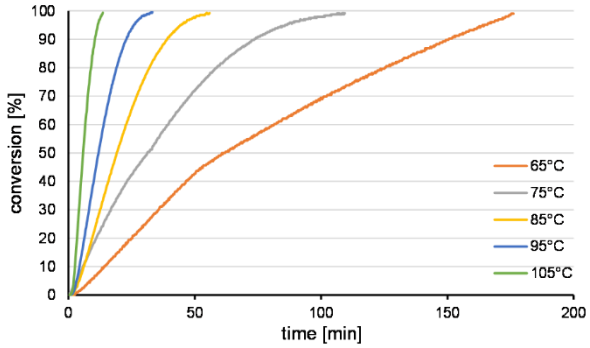

Figure 7 Pressure increase due to catalytic FA decomposition to CO2 and H2 as a function of time at different temperatures (65-105°C);

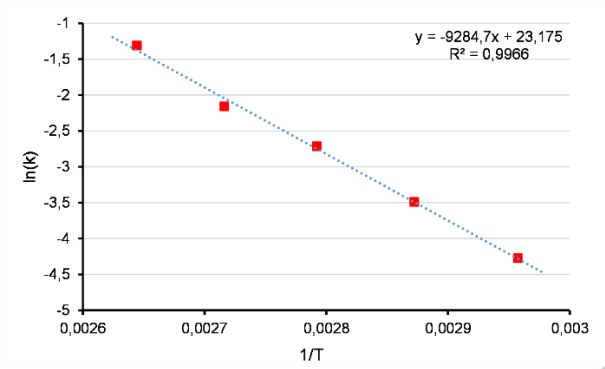

Figure 8 Arrhenius plot to determine the Ea; the necessary kinetic data was derived from pressure vs. time measurements;

Another important feature of a catalyst is the activation parameter, which was assessed via an Arrhenius plot (Figure 8). The kinetic curves of the reaction, recorded at different temperatures (Figure 7), were the experimental basis of our estimation. The apparent activation energy (E_a) was determined to be +77.19 ± 4 kJ/mol, which is in good agreement with other reported values for the iron catalyst [Fe(PP_3TS)] with +76.05 ± 7 kJ/mol, where PP_3TS is m-trisulfonated-tris[2-(diphenylphosphino)ethyl]phosphine sodium salt)[18c] and for the iridium-based catalyst [Cp*Ir(1,2-diaminocyclohexane)Cl]Cl)[16a] with 77.94 ± 3.2 kJ/mol. Also Esteruelas *et al*. reported a similar value for FA dehydrogenation with a trihydride-hydroxo-osmium(IV) species.[35]

We observed catalytic activity for selective FA dehydrogenation already at 55°C (TOF 15.2 h^{-1}), whereas the highest measured TOFs were reached at 105°C with 1085 turnovers per hour (Figure 9). The catalyst was tested towards its stability and reusability. Therefore, an aqueous solution with catalyst was prepared, and substrate was added, then the reaction was started by heating it up. This procedure was repeated for four times in a row. An increase of time until full conversion was reached would have been attributed to catalytic degradation. After four cycles, the conversion time did not increase and the catalyst performed at high TOFs (460.9 ± 11 at 95°C) throughout the recycling (Figure 10).

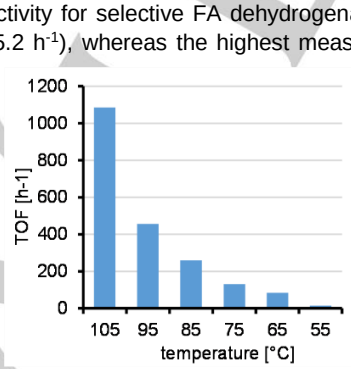

Figure 9 TOF h-1 at different temperatures

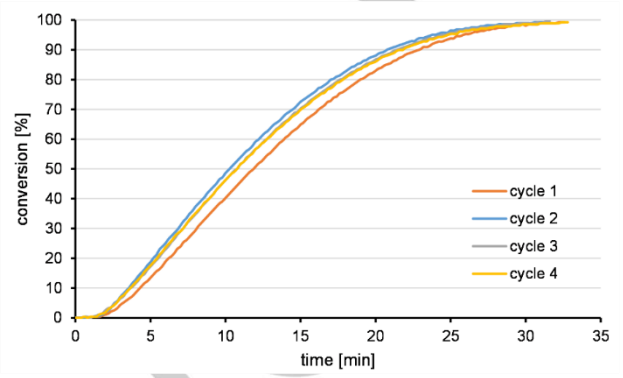

Figure 10 Recycling experiment at 95°C; the average time over four cycles to dehydrogenate 0.222 g FA was 32.05± 0.8 minutes; 8.3 mg catalyst in 1.778 g water

Based on our findings and in combination with literature data, [15d, 20b, 36] we reasoned the follow possible catalytic cycle for formic acid dehydrogenation (Figure 11).

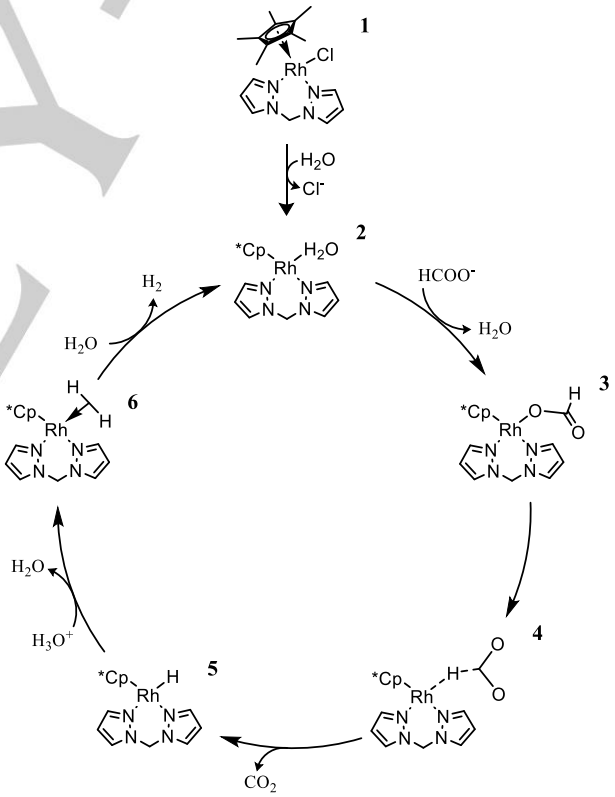

Figure 11 Suggested catalytic cycle for formic acid dehydrogenation

The precatalyst (**1**) enters the cycle by exchanging in an initial step chloride with water. This species (**2**) substitutes the coordinated water molecule with formate (**3**), which is linked via an oxygen atom. Direct hydride transfer leads to intermediate (**4**), where CO_2 is preformed and dissociates in the next step, forming hydride species (**5**) in this process. Next, a hydronium ion is stripped of a proton, yielding a free water molecule and coordinated non-classical dihydrogen (**6**). A water molecule

exchanges subsequently with the hydride, which is released as molecular dihydrogen and the initial aqua species (**2**) is regenerated.

Conclusions

In conclusion, the compound [Cp*Rh(dpm)Cl]Cl_2 was synthesized from $[Cp^*RhCl_2]_2$ and *bis(pyrazol-1-yl)methane*. The initial structure of the catalyst was confirmed by X-ray crystallography. The highly water-soluble precatalyst becomes active at low temperatures (55°C) for selective FA dehydrogenation and exhibits a turnover frequency of 1086 h^{-1} at 105°C (Figure 9). ^{1}H-NMR spectroscopy was employed to record the complete dehydrogenation of formic acid in the test tube and captured the process in a time-resolved stacked spectrum (Figure 5). The evaluation of this Rh complex also included the estimation of the activation parameter (+77.19 ± 4 kJ/mol), a value that was confirmed by literature findings. The recyclability of the catalyst at high temperatures (95°C) is on a stable level since in 4 cycles (3 recycles, Figure 10) no loss of activity was detected. An over-all observed issue with this type of structure seems to be the long-term stability at high temperatures and elevated H_2 pressures, resulting in a successive reduction of the metal centers and thereby to a partial deactivation, a phenomenon which was examined for an iridium congener by Prakash *et al*.[37]

Experimental Section

Materials
Solvents and chemicals were purchased from commercial suppliers and used without further purification. $RhCl_3(H_2O)_n$ (Rh: 37–42%) was obtained from Precious Metals Online (PMO Pty Ltd). All solvents had at least HPLC grade (for synthesis) or analytical grade (*p.a.*).

Instruments
Microwave syntheses were carried out with a Biotage Initiator 2.0 microwave synthesizer (400 W) in 20 mL microwave vials and equipped with magnetic stirring bars. NMR experiments were performed with a Bruker AV-400 (5 mm) for verification of the synthesized precatalyst while the kinetic measurements were recorded on a Bruker AVIII-400 in 10 mm medium pressure sapphire tubes.[34] MestReNova 11.0.2 was used for spectra analysis and evaluation.

Synthesis
bis(pyrazol-1-yl)methane (**1**)
The used synthetic method was published elsewhere by Jameson *et al*.[38] NMR see SI-Figure 2.

$[Cp^*RhCl_2]_2$ (**2**)
The synthetic method was published by Severin *et al*.[39] and applied with minor modifications by reducing the temperature from 145°C to 130°C and increasing the reaction time to 7 minutes (original 3 min). The yields are in the same range as reported. NMR see SI-Figure 3.

*[Cp*Rh(bis(pyrazol-1-yl)methane)Cl]Cl* (**3**)
90 mg $[Cp^*RhCl_2]_2$ (0.126 mmol) are dissolved in 2.5 mL DCM and 48 mg *bis(pyrazol-1-yl)methane* (2.1 eq.) are dissolved in 2.5 mL methanol. Then the two homogeneous transparent solutions are slowly combined; the reaction takes places immediately at room temperature and is indicated by a color shift of the Rh-containing solution from red to orange-yellow. After evaporating the solvent under reduced pressure, the compound was dissolved in a minimal amount of MeOH and precipitated with diethyl ether. The microcrystalline, pale orange powder was recovered by filtration over a frit, washed with ether and dried *in vacuo*. NMR see SI-Figure 4; mass spectrum SI-Figure 5.

Crystallization and X-ray diffraction
Single clear pale orange prism-shaped crystals of [Cp*Rh(bis(pyrazol-1-yl)methane)Cl]Cl were obtained by recrystallization from methanol at room temperature. A suitable crystal of 0.75×0.56×0.32 mm^3 was selected and mounted on a support on a SuperNova, Dual, Cu at home/near, AtlasS2 diffractometer. The crystal was kept at a steady temperature (140.01(10) K) during data collection. The structure was solved with the **ShelXT** (Sheldrick, 2015) structure solution program using the dual solution method and by using **Olex2** (Dolomanov et al., 2009) as the graphical interface. The model was refined with version 2018/3 of **ShelXL** (Sheldrick, 2015) using full matrix least squares on $|F|^2$ minimization.

Crystal Data
$C_{18}H_{27}Cl_2N_4ORh$, M_r = 489.24, orthorhombic, *Pca*2$_1$ (No. 29), a = 16.6621(2) Å, b = 7.14735(9) Å, c = 17.3205(2) Å, $\alpha = \beta = \gamma = 90^\circ$, V = 2062.69(5) Å^3, T = 140.01(10) K, Z = 4, Z' = 1, μ(MoKα) = 1.102, 44436 reflections measured, 7368 unique (R_{int} = 0.0337) which were used in all calculations. The final wR_2 was 0.0543 (all data) and R_1 was 0.0242 (I > 2(I)).
Summary of Data CCDC: 1905053

Procedure for formic acid dehydrogenation
Formic acid dehydrogenation experiments were performed as follows. A 10 mm sapphire NMR tube was charged with water-FA (pressure experiments) or deuterated water-FA (NMR) mixture (2.46 M). Then the catalyst was added (c(Rh) = 0,01 M), the tube was hermetically sealed and subjected to a heating source (heating jacket or NMR). The experiment was considered as over when there was no more pressure increase (pressure sensor) or the formic acid peak did no longer resonate in NMR measurements. When establishing the experimental procedure, the samples of the pressure experiments were conducted with D_2O as well and NMR was used to verify the level of FA dehydrogenation at the end of the pressure measurement (steady state).

Acknowledgments

École Polytechnique Fédérale de Lausanne (EPFL), Swiss National Science Foundation (Grant 200020_162351), Swiss Competence Center for Energy Research (SCCER), Swiss Commission for Technology and Innovation (CTI) are thanked for financial support.
We thank Euro Solari, Farzaneh Fadaei Tirani, and Rosario Scopelliti for resolving the crystal structure of the catalyst.

Keywords: formic acid, hydrogen, carbon dioxide utilization, formic acid dehydrogenation, hydrogen storage, homogeneous catalysis, pentamethylcyclopentadienyl, rhodium catalyst, sapphire tubes, Cp*Rh, bis(pyrazol-1-yl)methane, NMR spectroscopy, aqueous solution; crystal structure;

[1] M. O'NEILL, in *MailOnline*, Associated Newspapers Ltd, **2018**.
[2] a) T. R. Anderson, E. Hawkins, P. D. Jones, *Endeavour* **2016**, *40*, 178-187; b) P. Antti-Ilari, L. Martin, H. D. Matthews, *Environ. Res. Lett.* **2017**, *12*, 075002, doi.org/10.1088/1748-9326/aa98c9.
[3] a) A. F. Dalebrook, W. Gan, M. Grasemann, S. Moret, G. Laurenczy, *Chem. Commun. (Cambridge, U. K.)* **2013**, *49*, 8735-8751; b) M. Grasemann, G. Laurenczy, *Energy Environ. Sci.* **2012**, *5*, 8171-8181.
[4] N. Onishi, M. Iguchi, X. Yang, R. Kanega, H. Kawanami, Q. Xu, Y. Himeda, *Adv. Energy Mater.* **2018**, 1801275, doi.org/10.1002/aenm.201801275.
[5] Y. Yu, T. He, A. Wu, Q. Pei, A. Karkamkar, T. Autrey, P. Chen, *Angew. Chem., Int. Ed.* **2019**, *58*, 3102-3107.
[6] M. Chong, T. Autrey, C. M. Jensen, *Inorganics* **2017**, *5*, 89.
[7] M. D. Allendorf, Z. Hulvey, T. Gennett, A. Ahmed, T. Autrey, J. Camp, E. Seon Cho, H. Furukawa, M. Haranczyk, M. Head-Gordon, S. Jeong, A. Karkamkar, D.-J. Liu, J. R. Long, K. R. Meihaus, I. H. Nayyar, R.

Nazarov, D. J. Siegel, V. Stavila, J. J. Urban, S. P. Veccham, B. C. Wood, *Energy Environ. Sci.* **2018**, *11*, 2784-2812.
[8] a) K. Sordakis, C. Tang, L. K. Vogt, H. Junge, P. J. Dyson, M. Beller, G. Laurenczy, *Chem. Rev. (Washington, DC, U. S.)* **2018**, *118*, 372-433; b) C. Fellay, P. J. Dyson, G. Laurenczy, *Angew. Chem., Int. Ed.* **2008**, *47*, 3966-3968.
[9] K. Müller, K. Brooks, T. Autrey, *Energy Fuels* **2017**, *31*, 12603-12611.
[10] S. Moret, P. J. Dyson, G. Laurenczy, *Nat. Commun.* **2014**, *5, doi.org/10.1038/ncomms5017*.
[11] A. K. Singh, S. Singh, A. Kumar, *Catal. Sci. Technol.* **2016**, *6*, 12-40.
[12] K. Müller, K. Brooks, T. Autrey, *Energy Fuels* **2018**, *32*, 10008-10015.
[13] a) A. Iturmendi, L. Rubio-Pérez, J. J. Pérez-Torrente, M. Iglesias, L. A. Oro, *Organometallics* **2018**, *37*, 3611-3618; b) I. Mellone, N. Gorgas, F. Bertini, M. Peruzzini, K. Kirchner, L. Gonsalvi, *Organometallics* **2016**, *35*, 3344-3349; c) C. Chauvier, A. Tlili, C. Das Neves Gomes, P. Thuery, T. Cantat, *Chem. Sci.* **2015**, *6*, 2938-2942; d) E. A. Bielinski, P. O. Lagaditis, Y. Zhang, B. Q. Mercado, C. Würtele, W. H. Bernskoetter, N. Hazari, S. Schneider, *J. Am. Chem. Soc.* **2014**, *136*, 10234-10237; e) C. Prichatz, M. Trincado, L. Tan, F. Casas, A. Kammer, H. Junge, M. Beller, H. Grützmacher, *ChemSusChem.* **2018**, *11*, 3092-3095.
[14] a) J. J. A. Celaje, Z. Lu, E. A. Kedzie, N. J. Terrile, J. N. Lo, T. J. Williams, *Nat. Commun.* **2016**, *7*, 11308; b) Z. Wang, S.-M. Lu, J. Li, J. Wang, C. Li, *Chem.-Eur. J.* **2015**, *21*, 12592-12595; c) S. Wang, H. Huang, T. Roisnel, C. Bruneau, C. Fischmeister, *ChemSusChem.* **2019**, *12*, 179-184.
[15] a) M. Iglesias, L. Oro, *Eur. J. Inorg. Chem.* **2018**, *20-21*, 2125-2138; b) W.-H. Wang, M. Z. Ertem, S. Xu, N. Onishi, Y. Manaka, Y. Suna, H. Kambayashi, J. T. Muckerman, E. Fujita, Y. Himeda, *ACS Catal.* **2015**, *5*, 5496-5504; c) K. Sordakis, A. F. Dalebrook, G. Laurenczy, *ChemCatChem.* **2015**, *7*, 2332-2339; d) D. Zhang, X. Chen, H. Liu, X. Huang, *New J. Chem.* **2015**, *39*, 8060-8072; e) D. Mellmann, E. Barsch, M. Bauer, K. Grabow, A. Boddien, A. Kammer, P. Sponholz, U. Bentrup, R. Jackstell, H. Junge, G. Laurenczy, R. Ludwig, M. Beller, *Chem.-Eur. J.* **2014**, *20*, 13589-13602; f) W.-H. Wang, J. T. Muckerman, E. Fujita, Y. Himeda, *ACS Catal.* **2013**, *3*, 856-860.
[16] a) C. Fink, G. Laurenczy, *Dalton Trans.* **2017**, *46*, 1670-1676; b) E. Fujita, J. T. Muckerman, Y. Himeda, *BBA-BIOENERGETICS* **2013**, *1827*, 1031-1038; c) N. Onishi, S. Xu, Y. Manaka, Y. Suna, W.-H. Wang, J. T. Muckerman, E. Fujita, Y. Himeda, *Inorg. Chem.* **2015**, *54*, 5114-5123; d) W.-H. Wang, J. F. Hull, J. T. Muckerman, E. Fujita, Y. Himeda, *Energy Environ. Sci.* **2012**, *5*, 7923-7926; e) S. Xu, N. Onishi, A. Tsurusaki, Y. Manaka, W.-H. Wang, J. T. Muckerman, E. Fujita, Y. Himeda, *Eur. J. Inorg. Chem.* **2015**, *2015*, 5591-5594.
[17] G. van Koten, R. A. Gossage, *The Privileged Pincer-Metal Platform: Coordination Chemistry & Applications*, Springer International Publishing, **2015**.
[18] a) C. Federsel, A. Boddien, R. Jackstell, R. Jennerjahn, P. J. Dyson, R. Scopelliti, G. Laurenczy, M. Beller, *Angew. Chem., Int. Ed.* **2010**, *49*, 9777-9780; b) A. Boddien, D. Mellmann, F. Gärtner, R. Jackstell, H. Junge, P. J. Dyson, G. Laurenczy, R. Ludwig, M. Beller, *Science* **2011**, *333*, 1733-1736; c) M. Montandon-Clerc, A. F. Dalebrook, G. Laurenczy, *J. Catal.* **2016**, *343*, 62-67; d) T. Zell, D. Milstein, *Acc. Chem. Res.* **2015**, *48*, 1979-1994.
[19] G. A. Filonenko, R. van Putten, E. N. Schulpen, E. J. M. Hensen, E. A. Pidko, *ChemCatChem.* **2014**, *6*, 1526-1530.
[20] a) C. Fink, M. Montandon-Clerc, G. Laurenczy, *CHIMIA* **2015**, *69*, 746-752; b) N. Onishi, G. Laurenczy, M. Beller, Y. Himeda, *Coord. Chem. Rev.* **2017**.
[21] a) J. B. Curley, N. E. Smith, W. H. Bernskoetter, N. Hazari, B. Q. Mercado, *Organometallics* **2018**, *37*, 3846-3853; b) R. Watari, Y. Kayaki, S.-i. Hirano, N. Matsumoto, T. Ikariya, *Adv. Synth. Catal.* **2015**, *357*, 1369-1373; c) S. Oldenhof, J. I. van der Vlugt, J. N. H. Reek, *Catal. Sci. Technol.* **2016**, *6*, 404-408.
[22] C. Fink, S. Katsyuba, G. Laurenczy, *Phys. Chem. Chem. Phys.* **2016**, *18*, 10764-10773.
[23] W. Gan, P. J. Dyson, G. Laurenczy, *ChemCatChem.* **2013**, *5*, 3124-3130.
[24] Q.-L. Zhu, F.-Z. Song, Q.-J. Wang, N. Tsumori, Y. Himeda, T. Autrey, Q. Xu, *J. Mater. Chem. A* **2018**, *6*, 5544-5549.
[25] H. Zhong, M. Iguchi, M. Chatterjee, Y. Himeda, Q. Xu, H. Kawanami, *Adv. Sustainable Syst.* **2018**, *2*, 1700161.
[26] T. J. Kealy, P. L. Pauson, *Nature* **1951**, *168*, 1039.
[27] G. Wilkinson, *J. Am. Chem. Soc.* **1952**, *74*, 6146-6147.
[28] R. B. Moffett, *Org. Synth.* **1963**, *4*, 238.
[29] D. M. Morris, M. McGeagh, D. De Peña, J. S. Merola, *Polyhedron* **2014**, *84*, 120-135.
[30] J. F. Hull, Y. Himeda, W.-H. Wang, B. Hashiguchi, R. Periana, D. J. Szalda, J. T. Muckerman, E. Fujita, *Nature Chem.* **2012**, *4*, 383-388.
[31] a) K. Sordakis, A. Tsurusaki, M. Iguchi, H. Kawanami, Y. Himeda, G. Laurenczy, *Chem.-Eur. J.* **2016**, *22*, 15605-15608; b) K. Sordakis, A. Tsurusaki, M. Iguchi, H. Kawanami, Y. Himeda, G. Laurenczy, *Green Chem.* **2017**, *19*, 2371-2378.
[32] a) D. Evans, J. A. Osborn, G. Wilkinson, *J. Chem. Soc. A. Inorg. phys. theor.* **1968**, 3133-3142; b) S. Akutagawa, *Appl. Catal., A.* **1995**, *128*, 171-207; c) S. Fukuzumi, T. Kobayashi, T. Suenobu, *ChemSusChem.* **2008**, *1*, 827-834.
[33] S. H. Strauss, K. H. Whitmire, D. F. Shriver, *J. Organomet. Chem.* **1979**, *174*, C59-C62.
[34] S. Moret, P. J. Dyson, G. Laurenczy, *Dalton Trans.* **2013**, *42*, 4353-4356.
[35] M. A. Esteruelas, C. García-Yebra, J. Martín, E. Oñate, *ACS Catal.* **2018**, *8*, 11314-11323.
[36] L. M. A. Quintana, S. I. Johnson, S. L. Corona, W. Villatoro, W. A. Goddard, M. K. Takase, D. G. VanderVelde, J. R. Winkler, H. B. Gray, J. D. Blakemore, *Proc. Natl. Acad. Sci. U. S. A.* **2016**, *113*, 6409-6414.
[37] M. Czaun, J. Kothandaraman, A. Goeppert, B. Yang, S. Greenberg, R. B. May, G. A. Olah, G. K. S. Prakash, *ACS Catal.* **2016**, *6*, 7475-7484.
[38] M. R. Churchill, D. G. Churchill, M. H. V. Huynh, K. J. Takeuchi, R. K. Castellano, D. L. Jameson, *J. Chem. Crystallogr.* **1996**, *26*, 93-97.
[39] J. Risse, B. Dutta, E. Solari, R. Scopelliti, K. Severin, *Z. Anorg. Allg. Chem.* **2014**, *640*, 1322-1329.

10.1002/ejic.201900344

WILEY-VCH

Entry for the Table of Contents (Please choose one layout)

Layout 1:

FULL PAPER

Text for Table of Contents

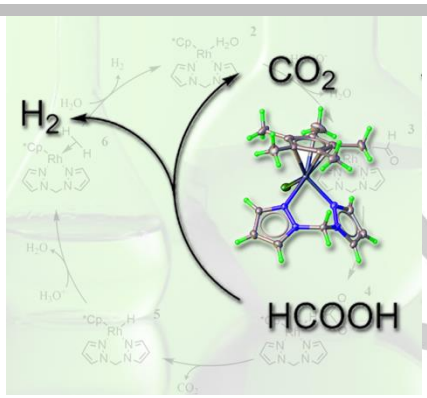

Cornel Fink and Gábor Laurenczy**

Page No. – Page No.

A precious catalyst: Rhodium-catalyzed formic acid dehydrogenation in water